

Clean-limit pair breaking and two-dimensional vortex dynamics in ferromagnet-superconductor heterostructures

K. Senapati and R. C. Budhani

Department of Physics, Indian Institute of Technology Kanpur, Kanpur—208016, India

(Received 29 July 2004; published 12 November 2004)

Superconductivity in $\text{YBa}_2\text{Cu}_3\text{O}_7$ films of thickness $d_Y < 500 \text{ \AA}$ sandwiched between ferromagnetic and nonmagnetic epitaxial layers has been probed. The irreversibility temperature $T_{\text{irr(H)}}$ in the vortex state maps onto a clean-limit pair-breaking temperature $T_{\text{c(H)}}$, and a universal relation exists between the pair-breaking field H_{pb} and an effective thickness $d_{\text{eff}} (< d_Y)$ of the superconductor. The vortex response in these two-dimensional (2D) films indicates a crossover temperature T^* , which separates two regimes of flux motion controlled by formation of dislocations ($T > T^*$), and migration of preexisting dislocations and dislocation pairs ($T < T^*$) in the 2D flux line lattice.

DOI: 10.1103/PhysRevB.70.174506

PACS number(s): 74.78.Fk, 74.25.Qt, 74.62.Yb, 74.78.Bz

The coexistence of ferromagnetism and superconductivity, the two antagonistic quantum phenomena,¹ has gained renewed interest in recent years.^{2–5} This spur in activity is a compound effect of the ability to realize well-controlled growth of superconducting (SC)/ferromagnetic (FM) superlattices, the discovery of new compounds which show exotic superconductivity and magnetism, and the search for spintronics and quantum computing related devices. The issues of fundamental interest in this area have been a π phase-shifted SC order parameter in the ferromagnetic layer,² the exchange coupling between two FM layers separated by a thin SC film,³ spin polarized quasiparticle dynamics in the superconductor, etc.^{4,5}

An important but rarely addressed issue in such FM/SC/FM sandwiches is the vortex state of the nearly two-dimensional SC layer. It has been shown that the interaction between two vortices separated by a distance r in the range $\xi(T) \ll r \ll \Lambda(T)$ is $V(r) \approx -(\phi_0^2/4\pi^2\Lambda)\ln(r/\xi)$, where $\Lambda(T) = 2\lambda_B^2(T)/d$ is the effective magnetic penetration depth in a film of thickness $d \ll \lambda_B$, penetration depth in the bulk, and $\xi(T)$ is the coherence length.^{6,7} Thus, as long as the intervortex spacing $a_0 = (\phi_0/H)^{1/2} \ll \Lambda(T)$, the nearest-neighbor interaction is logarithmic in separation a_0 . In the limit $T \sim 0$, this long-range interaction leads to a 2D flux line lattice (FLL), which melts via copious nucleation of dislocations at $T = T_m$, where T_m is the melting temperature. However, frozen-in disorder changes the dynamics of the vortex state in a nontrivial manner. While for a 3D-FLL a vortex glass phase is predicted in which the barriers for vortex motion diverge with the decreasing driving force, in 2D such behavior is expected only in the limit of $T \approx 0$.⁸ In the backdrop of this prediction, it becomes important to address how the presence of FM boundaries would affect the FLL dynamics in 2D superconductors. *A priori*, one expects the FM boundaries to suppress the condensate density by pair breaking and hence reduce intervortex interaction. However, it has also been argued that the FM boundaries can promote pinning of the magnetic flux of vortices.⁹ Indeed, ordered arrays of submicron-size magnetic dots on Nb films lead to strong pinning of vortices.¹⁰

In this paper we report vortex dynamics in thin $\text{YBa}_2\text{Cu}_3\text{O}_7$ (YBCO) films sandwiched between FM layers

of $\text{La}_{0.67}\text{Sr}_{0.33}\text{MnO}_3$ (LSMO). In order to separate out the magnetic contribution, we have also measured the response of YBCO films with boundaries of $\text{PrBa}_2\text{Cu}_3\text{O}_7$ (PBCO). We note that the singular effect of FM boundaries is to suppress T_c through pair breaking over a critical thickness $\xi_c \approx 20 \text{ \AA}$. The field-temperature (H - T) phase boundary above which pinning-dominated dynamics of the FLL becomes irrelevant can be identified with a clean-limit pair-breaking temperature $T_{\text{c(H)}}$. Our ac susceptibility technique allows measurements of FLL dynamics deep in the H - T phase space, which is not accessible to standard resistivity measurements. We identify the crossover temperature T^* that separates two regimes of thermally activated flux flow (TAFF) associated with the formation of dislocations, and migration of preexisting dislocations and dislocation pairs in 2D-FLL. The characteristic energy of these processes scales with the effective thickness of the superconducting film.

LSMO/YBCO/LSMO (FM/SC/FM) and PBCO/YBCO/PBCO (NM/SC/NM) trilayers were deposited on chemically polished¹¹ SrTiO_3 substrates with pulsed laser ablation. A slow deposition rate ($\sim 1 \text{ \AA/s}$) was used to realize a layer-by-layer growth of LSMO (300 \AA), PBCO (100 \AA), and YBCO (50 to 500 \AA). The SC and FM critical temperatures of the films were established through resistivity $\rho(T)$ and magnetization $M(T)$ measurements. For studies of vortex dynamics, we have used a miniature Hall probe-based ac susceptometer, details of which are published elsewhere.¹² The dc and ac magnetic fields in this setup are collinear and perpendicular to the plane of the $3 \times 3 \text{ mm}^2$ thin film sample. The experiment involved measurements of in-phase (T'_H) and quadrature (T''_H) components of the fundamental transmittivity.^{13,14} The onset of nonlinear response is measured by monitoring the third harmonic signal T_{H3} . In the weak screening regime, where the penetration depth λ_{ac} of the ac field is greater than the sample size, the fundamental transmittivity T'_H is related to the sheet inductance L of the superconducting film as $T'_H = 1 - (4\pi a^2/c^2 dL)$.¹⁴ Here, d and a are film thickness and effective radius of the film, respectively, and L is related to the impedance Z of the film as $1/L = \omega \text{Im}(1/Z)$. If the vortex motion in the weak pinning regime is thermally activated, one expects $1/L$ to show Arrhenius behavior.

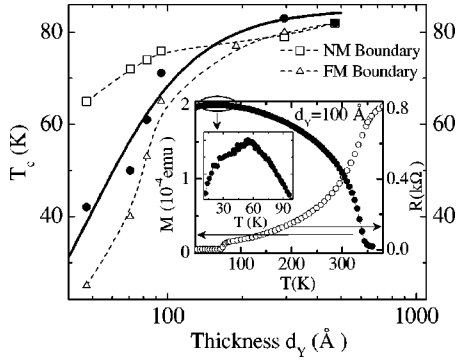


FIG. 1. T_c (open symbols) plotted as a function of d_Y in FM/SC/FM and NM/SC/NM trilayers. Filled circles in the figure represent the calculated T_c [defined as $T_c(d_Y) = T_{c(0)} - [\Delta T_c(d_Y)]_{\text{total}} + [\Delta T_c(d_Y)]_{\text{interface}}$]. Here, $T_{c(0)}$ is the T_c of 500 Å thick YBCO (82 K). This expression represents the critical temperature only under the influence of the pair-breaking field of LSMO. Solid line is a fit to the pair-breaking theory (Ref. 20). Inset shows $R(T)$ and zero-field cooled $M(T)$ of a FM/SC/FM sample with $d_Y = 100$ Å. An enlarged view of $M(T)$ near T_c is also shown.

In Fig. 1 we show the variation of T_c with the thickness of YBCO film (d_Y). The critical temperature of our NM/SC/NM sandwiches is consistent with earlier measurements of T_c on similar structures prepared by PLD and magnetron sputtering.¹⁵ Various reasons have been given for the observed drop in T_c as d_Y is reduced.^{15,16} These include interfacial stress, a drop in c -axis coupling of the condensate as the number of CuO_2 planes is reduced, and nonuniform changes in the interatomic distances of YBCO layers which lower the hole concentration. However, the effect of uniaxial pressure applied along the a and b axis of a YBCO crystal on its T_c is nearly equal and opposite.¹⁷ This result rules out any direct effect of a lattice mismatch-induced stress on T_c .

The onset of the FM and SC orders in the FM/SC/FM heterostructures on cooling below 350 K is clearly seen in $R(T)$ and $M(T)$ data (see the inset of Fig. 1).¹⁸ We notice a much sharper drop in the T_c with the decreasing d_Y in this case. Such suppression of T_c has been observed in other manganite-cuprate heterostructures as well.¹⁹ The suppression of T_c [$(\Delta T_c)_{\text{total}}$] here is a compound effect of the processes operating in the case of PBCO-YBCO-PBCO system [$(\Delta T_c)_{\text{interface}}$] and the pair-breaking effects of the magnetic layers [$(\Delta T_c)_{\text{pb}}$]. If we assume that the interface effects are identical in the two cases, we can express the effect of pair breaking alone on T_c as $(\Delta T_c)_{\text{pb}} = (\Delta T_c)_{\text{total}} - (\Delta T_c)_{\text{interface}}$. Using this procedure, we have plotted the effective T_c of the FM/SC/FM structures as a function of d_Y . The solid line in the figure is a fit to the equation $\ln(T_{c(0)}/T_c) = \chi(\pi^2 \xi_c^2 / 4d_Y)$, where $\chi(z) = \psi(1/2 + z/2) - \psi(1/2)$, $T_{c(0)}$ the transition temperature of 500 Å thick YBCO, ξ_c the boundary layer thickness over which T_c is reduced to zero, and ψ the digamma function. This expression is derived²⁰ from the de Gennes-Werthamer theory of proximity coupling and the Abrikosov-Gorkov model for pair breaking by magnetic impurities. The fitting (Fig. 1) yields a $\xi_c \sim 20$ Å. This simple picture allows us to define the effective thickness d_{eff} of the superconductor in the ferromagnetic sandwiches relative to the NM/SC/NM trilayers as $d_{\text{eff}} = d_Y - 2\xi_c$.

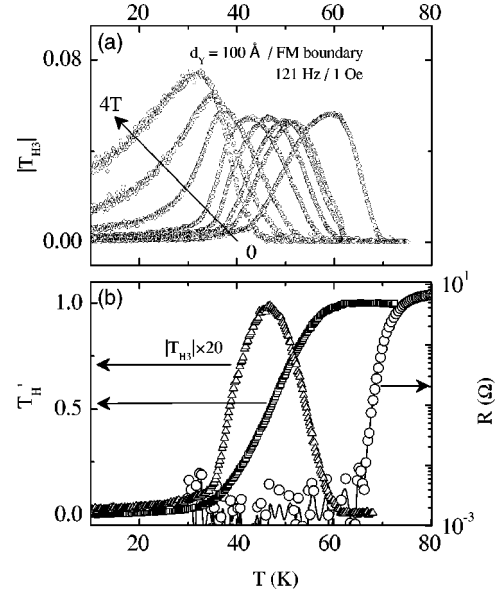


FIG. 2. Panel (a) shows T_{H3} measured at 121 Hz ($H_{ac} = 1.0$ Oe) as a function of temperature for a FM/SC/FM trilayer with $d_Y = 100$ Å at several values of dc magnetic field ($H_{dc} = 0, 1, 2, 5, 10, 20, 30,$ and 40 kOe). Panel (b) compares $T_{H'}$, T_{H3} , and $R(T)$ of the film of panel (a) at $H_{dc} = 5$ kOe.

In Fig. 2(a) we show the T_{H3} of a $d_Y = 100$ Å film with FM boundaries measured at 121 Hz. The onset of T_{H3} on cooling from the normal state signals a nonlinear response of vortices to the applied driving force.¹⁴ It is certainly ω -dependent, and in the limit of $\omega \sim 0$, the temperature of onset is the irreversibility temperature $T_{\text{irr}(H)}$. It is interesting to note that the appearance of T_{H3} coincides with the temperature at which $T_{H'}$ starts to decrease from unity [Fig. 2(b)]. Measurements of $T_{H'}$ yield the linear component of the response of a vortex manifold in which pinning interactions are relevant. The fact that $T_{H'}$ does not represent the pure Bardeen-Stephen-type flux flow becomes clear from Fig. 2(b) where we compare the $R(T)$, T_{H3} , and $T_{H'}$. The T_{H3} appears (correspondingly $T_{H'}$ falls from unity) when $R(T)$ drops by $\sim 10^4$ from its normal state value. The zero-frequency limit of $T_{\text{irr}(H)}$, therefore, can be identified as $T_{c(H)}$, the critical temperature at which λ_{ac} diverges and pinning becomes irrelevant.

The loss of pinning amounts to a loss of condensate stiffness due to magnetic-field-assisted phase fluctuations and pair breaking. A simple orbital pair-breaking scenario leads to $\ln[T_{c(H)}/T_c] = -\pi\alpha/4k_B T_{c(H)}$, where the energy α is related to pair breaking rate $(\tau_k)^{-1}$ as $2\alpha = \hbar/\tau_k$.^{21,22} For a thin sample placed in a perpendicular magnetic field, the phase of the order parameter changes by unity over the magnetic length scale $l_H = (\phi_0/2\pi H)^{1/2}$. Since high- T_c cuprates are in the clean limit,²³ the quasiparticle dynamics is expected to be ballistic over length l_H even at a dilute flux density. This leads to $\tau_k^{-1} = v_F/l_H = v_F(2\pi H/\phi_0)^{1/2}$ and $\ln[T_{c(H)}/T_c] = -(2\pi)^{1/2} \hbar v_F / 8k_B \sqrt{\phi_0}; (H)^{1/2}/T_{c(H)}$, where v_F is the Fermi velocity. The inset of Fig. 3 displays the variation of $T_{c(H)}/T_c$ with H . In the main panel of Fig. 3 we show a plot of $\ln[T_{c(H)}/T_c]$ vs $H^{1/2}/T_{c(H)}$ for four samples of different

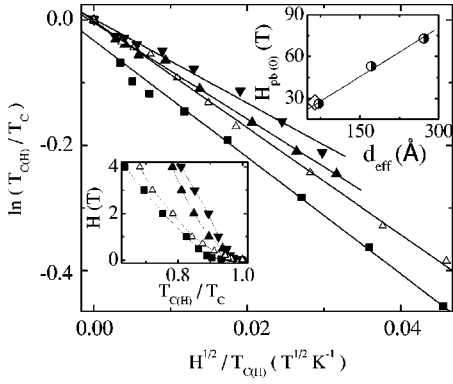


FIG. 3. $\ln(T_{c(H)}/T_c)$ plotted as a function of $H^{1/2}/T_{c(H)}$ for YBCO films with FM boundaries (\blacksquare —100 Å, \blacktriangle —200 Å, and \blacktriangledown —300 Å) and NM boundaries (\triangle —100 Å). Lower inset shows plot of irreversibility field vs $T_{c(H)}/T_c$. Upper inset shows the pair-breaking field $H_{pb(0)}$. The $H_{pb(0)}$ of the films with NM boundaries is represented by the symbol \diamond .

thickness. A linear dependence, irrespective of the nature of the boundaries is evident in all cases at $H > 5$ kOe. Following Hebard *et al.*²² we have calculated the pair-breaking field $H_{cp(0)}$. The upper inset of Fig. 3 shows $H_{cp(0)}$ plotted as a function of d_{eff} . A universal relation, independent of other details such as film thickness and film boundary, exists between $H_{cp(0)}$ and T_c in these ultrathin films.

Figure 4 shows the plots of $\log_{10} T'_H$ vs $1/T$ for $d_Y = 75$ Å with LSMO [Fig. 4(a)] and PBCO [Fig. 4(b)] boundaries. Here, it needs to be recognized that the range of tem-

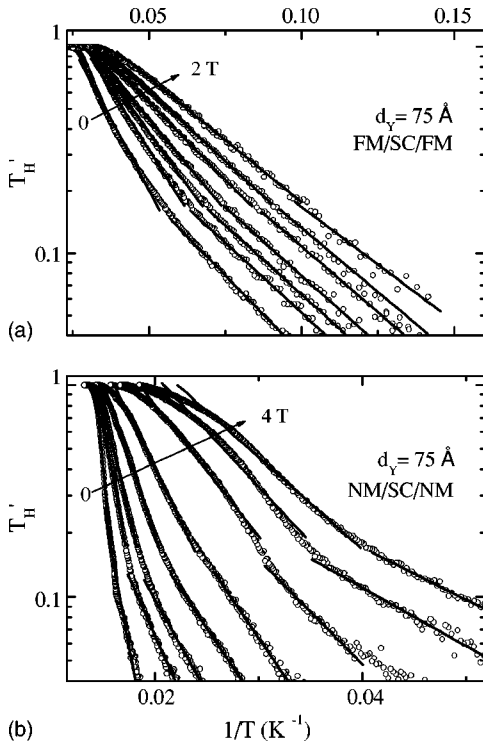


FIG. 4. Panel (a) shows $\log_{10} T'_H$ vs $1/T$ plot for a $d_Y = 75$ Å film with the FM boundaries. The fundamental transmittivity of a $d_Y = 75$ Å film with the PBCO boundaries is shown in panel (b).

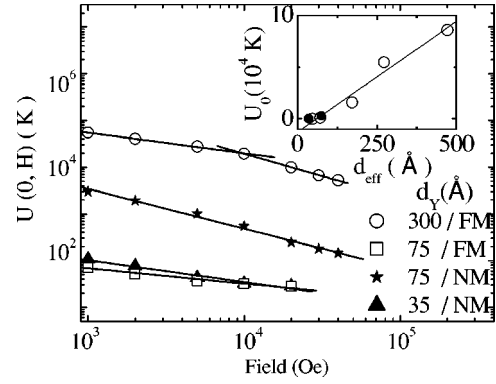


FIG. 5. Activation energy $U_0(0)$ plotted as a function of H_{dc} for films with FM and NM boundaries. The $U_0(0)$ was calculated from the slope of $\log_{10} T'_H$ vs $1/T$ plots (Fig. 4) for $0.2 \leq T'_H \leq 0.8$. Inset shows the activation energy at 1 kOe for several films as a function of $d_{eff}(d_Y - 2\xi_c)$. Note that $\xi_c = 0$ for the films with NM boundaries. The $U_0(0)$ of these films is shown by closed symbols in the inset.

perature being probed by the T'_H data is below $T_{irr(H)}$. We note that while the $\log_{10} T'_H$ vs $1/T$ plots for the range of $0.9 > T'_H > 0.15$ can be approximated by a straight line, a distinct change in the slope is seen at a critical temperature T^* , where T'_H falls below ≈ 0.15 . This indicates a crossover to a different regime of dynamics at lower temperatures ($T < T^*$). Interestingly, the $\log_{10} T'_H$ vs $1/T$ plots of thick films (> 300 Å) are characterized by a single activation energy down to the lowest temperature without any indications of a T^* .

In Fig. 5 we plot the activation energy $U_0(0)$ above T^* in the limit $T=0$ following a dependence of the type $U_0(T) \sim U_0(0)(1 - T/T_c)$, derived from the T dependence of the shear modulus ($c_{66} \sim 1/\lambda_B^2$) of the FLL.^{6,24} There are three noteworthy features of these data: (i) for the same d_Y , $U_0(0)$ of the FM/SC/FM trilayer is much smaller than the $U_0(0)$ of the NM/SC/NM layer; (ii) for $d_Y < 200$ Å, $U_0(0)$ shows a $\sim \ln(1/H)$ dependence; and (iii) the $U_0(0)$ scales with the effective thickness of the SC layer $d_{eff}(=d_Y - 2\xi_c)$. The scaling of $U_0(0)$ with d_{eff} at 1 kOe is evident in the inset of Fig. 5. Note that the data for NM/SC/NM films also fall on the same curve. The $U_0(0)$ of thicker films shows a deviation from $\ln(1/H)$ dependence at the higher fields. This is a signature of field induced 2D-to-3D crossover in the FLL.²⁵

The observation of two activation energies agrees with the prediction of Feigelman, Geshkenbein, and Larkin for thermally activated plastic motion of vortices in 2D-FLL with weak pinning.²⁴ Since the energy cost of moving a pinned vortex is much more than the energy required to create and then move a 2D dislocation, the vortex motion at $T \sim T_m$ proceeds via nucleation and subsequent motion of dislocations over the pinning barriers. The dissipation is characterized by a resistivity $\rho_d = \rho_f v_0 \exp[-\Delta \varepsilon_p^d / T] \cdot n_d R_1^2$, where ρ_f is the flux flow resistivity, v_0 the characteristic attempt frequency, $\Delta \varepsilon_p^d$ the pinning barrier for dislocations, n_d the dislocation density, and $R_1 = (R_c^2 + R_0^2)^{1/2}$, the length scale over which two dislocations interact. Here, R_c is the collective pinning length and R_0 the radius of the flux bundle, which moves by ξ when the dislocation is displaced by unit lattice

spacing a_0 . Since pinning is strong in thin films of YBCO (small R_c), we can write $R_1 \sim R_0$. The number density of dislocations at T is $n_d(T) \sim \exp[-(\varepsilon_d/2T)\ln(R_0/a_0)]$, where $\varepsilon_d = c_{66}da_0^2/\pi$. For a YBCO film of thickness $d_Y = 300$ Å and $\lambda(0) = 1400$ Å, $\varepsilon_d \approx 10^4$ K, in agreement with the data shown in Fig. 5. In the region of 2D collective pinning, $\Delta\varepsilon_p^d \ll \varepsilon_d$. Hence, at sufficiently high temperatures, the $U_0(T)$ for dissipation is essentially the energy required to create a dislocation, which is $\varepsilon_d \ln(R_0/a_0) = \varepsilon_d \ln(a_0/\xi) \sim \varepsilon_d \ln(H_{c2}/H)$. The field dependence of the $U_0(0)$ shown in Fig. 5 is in agreement with this prediction. Further, the scaling of the $U_0(0)$ with the d_{eff} is embodied in the relation $\varepsilon_d = c_{66}da_0^2/\pi$, as long as the vortices are correlated along the entire thickness d of the film.

At lower temperatures, where the thermal activation is not large enough to create free dislocations, the motion of disorder-induced dislocations existing in the FLL at $T=0$ leads to dissipation. The upper limit for the energy required to move the dislocations in YBCO films is $\approx 10^3$ K.²⁵ Another mechanism for plastic TAFF at $T \ll T_m$ is the motion of small dislocation pairs.²⁴ Both these mechanisms will contribute to a T -dependent activation energy $U_0(T)$, which is smaller than ε_d . Examples of such behavior abound in nature. In ionic solids, for example, the migration of preexisting Schottky and Frenkel defects leads to a low-temperature thermally activated ionic conductivity.²⁶ Here, it needs to be emphasized that while a $\ln(1/H)$ -dependent activation energy has been seen in $\rho_f(T)$ of quasi-2D $\text{BiSr}_2\text{CaCu}_2\text{O}_8$,²⁷

high- T_c superlattices²⁸ and amorphous alloy thin films,²⁹ the $\rho_f(T)$ measurements are not sensitive enough to probe the low-temperature dynamics seen here. Recent mutual inductance measurements of Calame *et al.*³⁰ on thin YBCO films reveal a change in dynamics at lower temperatures, which the authors identify with vortex excitations over the lowest energy barriers of a pinning-potential landscape. However, the magnitude of this barrier has not been calculated.

In summary, we have studied the dynamics of the mixed state in 2D films of YBCO sandwiched between FM boundaries over a broad range of temperature and vortex density. These studies reveal two distinct regimes of thermally activated dissipation deep in the H - T phase space. Our observations are in excellent agreement with the theory of dislocation mediated plastic TAFF in 2D-FLL. The characteristic energy of these processes scales with the effective thickness $d_{\text{eff}} = d_Y - 2\xi_c$ of the superconductor. It is interesting to note that all effects of the FM boundaries on the mixed state are embodied in the critical thickness ξ_c over which superconductivity is quenched by pair breaking.

We thank Lance Cooley, R. L. Greene, Deepak Kumar, Qiang Li, C. J. Lobb, S. B. Ogale, Myron Strongin, M. Suenaga, and D. O. Welch for their critical comments on this work. The support for this research has come from the Defense Research and Development Organization, Government of India.

¹H. Suhl, *J. Less-Common Met.* **62**, 225 (1978).

²A. I. Buzdin, L. N. Bulaevski, and S. V. Panyukov, *JETP Lett.* **35**, 178 (1982); V. V. Ryazanov, V. A. Oboznov, A. Yu. Rushanov, A. V. Veretennikov, A. A. Golubov, and J. Aarts, *Phys. Rev. Lett.* **86**, 2427 (2001); Y. Blum, A. Tsukernik, M. Karpovskii, and A. Palevski, *ibid.* **89**, 187004 (2002).

³O. Šipr and B. L. Györfy, *J. Phys.: Condens. Matter* **7**, 5239 (1995); C. A. R. Sá de Melo, *Phys. Rev. Lett.* **79**, 1933 (1997).

⁴A. G. Aronov, *Sov. Phys. JETP* **44**, 193 (1976).

⁵V. A. Vas'ko, V. A. Larkin, P. A. Kraus, K. R. Nikolaev, D. E. Grupp, C. A. Nordman, and A. M. Goldman, *Phys. Rev. Lett.* **78**, 1134 (1997); Z. W. Dong, R. Ramesh, T. Venkatesan, M. Johnson, Z. Y. Chen, S. P. Pai, V. Taliansky, R. P. Sharma, R. Shreekala, C. J. Lobb, and R. L. Greene, *Appl. Phys. Lett.* **71**, 1718 (1997); N.-C. Yeh, R. P. Vasquez, C. C. Fu, A. V. Samoilov, Y. Li, and K. Vakili, *Phys. Rev. B* **60**, 10 522 (1999).

⁶D. S. Fisher, *Phys. Rev. B* **22**, 1190 (1980).

⁷B. I. Halperin and D. R. Nelson, *J. Low Temp. Phys.* **36**, 599 (1979).

⁸M. P. A. Fisher, *Phys. Rev. Lett.* **62**, 1415 (1989); D. S. Fisher, M. P. A. Fisher, and D. A. Huse, *Phys. Rev. B* **43**, 130 (1991).

⁹S. Takahashi and M. Tachiki, *Phys. Rev. B* **35**, 145 (1987); L. N. Bulaevskii, E. M. Chudnovski, and M. P. Maley, *Appl. Phys. Lett.* **76**, 2594 (2000).

¹⁰J. I. Martín, M. Veléz, J. Nogués, and I. K. Schuller, *Phys. Rev. Lett.* **79**, 1929 (1997).

¹¹M. Kawasaki, K. Takahashi, T. Maeda, R. Tsuchiya, M. Shino-

hara, O. Ishiyama, T. Yonezawa, M. Yoshimoto, and H. Koinuma, *Science* **266**, 1540 (1994).

¹²K. Senapati, S. Chakravarty, L. K. Sahoo, and R. C. Budhani, *Rev. Sci. Instrum.* **75**, 141 (2004).

¹³J. Gilchrist, and M. Konczykowski, *Physica C* **212**, 43 (1993).

¹⁴C. J. van der Beek, M. Konczykowski, V. M. Vinokur, G. W. Crabtree, T., W. Li, and P. H. Kes, *Phys. Rev. B* **51**, 15492 (1995).

¹⁵J.-M. Triscone and Ø. Fischer, *Rep. Prog. Phys.* **60**, 1673 (1997), and references therein.

¹⁶M. Varela, Z. Sefriovi, D. Arias, M. A. Navacerrada, M. Lucia, M. A. Lopez de la Torre, C. Leon, G. D. Loss, F. Sanchez-Quesada, and J. Santamaria, *Phys. Rev. Lett.* **83**, 3936 (1999); T. Terashima, K. Shimura, Y. Bando, Y. Matsuda, A. Fujiyama, and S. Komiyama, *ibid.* **67**, 1362 (1991).

¹⁷W. E. Pickett, *Phys. Rev. Lett.* **78**, 1960 (1997).

¹⁸Unlike the other double-exchange ferromagnets, LSMO with ($x = 0.33$) is a metal in the paramagnetic state. This metallic behavior is observed in our LSMO films of $d_{\text{LSMO}} > 100$ Å. The resistivity of these films at 2 K is ~ 100 $\mu\Omega$ cm. Both these features indicate growth of a high-quality thin film.

¹⁹G. Jacob, V. V. Moshchalkov, and Y. Bruynseraede, *Appl. Phys. Lett.* **66**, 2564 (1995); Z. Sefriovi, M. Varela, V. Pena, D. Arias, C. Leon, J. Santamaria, J. E. Villegas, J. L. Martinez, W. Saldoiriaga, and P. Prieto, *ibid.* **81**, 4568 (2002); H.-U. Habermeier, G. Cristiani, R. K. Kremer, O. Lebedev, and G. van Tendeloo, *Physica C* **364–365**, 298 (2001); B. S. H. Pang, R. I.

- Tomov, and M. G. Blamire, *Supercond. Sci. Technol.* **17**, 624 (2004).
- ²⁰J. J. Hauser, H. C. Theuerer, and N. R. Werthamer, *Phys. Rev.* **142**, 118 (1966).
- ²¹M. Tinkham, *Introduction to Superconductivity* (Krieger, Malabar, FL, 1980), p. 264.
- ²²A. F. Hebard, P. L. Gammel, C. E. Rice, and A. F. J. Levi, *Phys. Rev. B* **40**, 5243 (1989).
- ²³M. Gurvitch and A. T. Fiory, *Phys. Rev. Lett.* **59**, 1337 (1987).
- ²⁴M. V. Feigel'man, V. B. Geshkenbein, and A. I. Larkin, *Physica C* **167**, 177 (1990).
- ²⁵G. Blatter, M. V. Feigel'man, V. B. Geshkenbein, A. I. Larkin, and V. M. Vinokur, *Rev. Mod. Phys.* **66**, 1125 (1994).
- ²⁶C. Kittel, *Introduction to Solid State Physics*, 7th ed. (Wiley, New York, 1996), p. 541.
- ²⁷T. T. M. Palstra, B. Batlogg, R. B. van Dover, L. F. Schneemeyer, and J. V. Waszczak, *Phys. Rev. B* **41**, 6621 (1990).
- ²⁸Y. Suzuki, J.-M. Triscone, M. R. Beasley, and T. H. Geballe, *Phys. Rev. B* **52**, 6858 (1995).
- ²⁹W. R. White, A. Kapitulnik, and M. R. Beasley, *Phys. Rev. Lett.* **70**, 670 (1993).
- ³⁰M. Calame, S. E. Korshunov, Ch. Leemann, and P. Martinoli, *Phys. Rev. Lett.* **86**, 3630 (2001).